COMPARISON BETWEEN EXPERIMENTAL AND NUMERICAL RESULTS OF FLOOD FLOW IN A COMPOUND MEANDERING CHANNEL

Alex George Mutasingwa, Graduate student, Hiroshima University
Shoji Fukuoka, Professor, Department of Civil and Env. Eng., Hiroshima University
Akihide Watanabe, Ass. Professor, Department of Civil and Env. Eng., Hiroshima University
(1-4-1, Kagamiyama, Higashi Hiroshima, 739, Japan; Tel./Fax; +81-824-24-7821)

While numerous steady compound channel flow studies have been conducted, unsteady compound channel flow has received relatively little attention. This paper presents a comparison between 2-dimensional unsteady flow numerical model and experimental results for flow variables in a compound meandering channel. Extensive flood flow experimental data obtained from a compound meandering channel experiments in the Hydraulic Laboratory, Hiroshima University is used for comparison with the numerical model. The numerical method is based on a finite volume discretization on a staggered grid with upwind scheme in flux, it handles drying and wetting process for a flood plain, has the ability to handle complex geometry and discontinuities, which are the main requirements for modeling compound channel flows. Comparison between measured data and model simulations show generally good agreement. This shows how useful the model can be in prediction of flood propagation in channels.

Key word: unsteady flow, compound meandering channel and numerical computation

1. INTRODUCTION

Various laboratory and numerical investigations were performed to study flow phenomenon in open channels, in most of these studies, steady flow investigations have been done (ASCE T.C, 1996; Fukuoka et. al, 1998; Sofialidis and Prinos, 1998; Zhao et. al 1994). Zhao et. al, 1994 observed that existing 2-dimensional numerical models have limited range of applicability in which they were developed. This results in uncertainty of computational results when the 2-dimensional model is applied outside its basic simulation features. From this viewpoint, water resources engineers, river and hydraulic engineers still demand reasonably reliable and accurate 2-dimensional dynamic models for practical engineering planning and designs.

Unsteady flow in a multistage channel involves a stage in which the flow overtops the bank and inundates the flood plain so that part of the flow is carried by the flood plains. The relative depth varies from zero at bankful to some value depending on the discharge hydrograph. Low relative depths are associated with large velocity difference between main channel and flood plain that results to lateral momentum transfer across the interface between main channel and flood plain (Wormleaton et. al, 1990). To quantify this lateral flow exchange in one-dimensional models, weir equations are normally used (Cunge et. al, 1980; Kun-Yeun et. al, 1998), or apparent shear stress computation approach (Fukuoka et. al, 1990; Wormleaton et. al, 1990). However, these approaches have some uncertainties on the choice of weir discharge coefficients (Shome et. al, 1990) and determination of mixing coefficients in the apparent shear stress approach.

This paper presents a comparison between unsteady flow laboratory experimental results and 2-dimensional numerical simulations. It describes an improved numerical model, which was

developed earlier by Nagata et. al, 1999. The original Nagata's approach could not simulate well laboratory unsteady compound meandering channel flow results. Two major items of the method were modified; the way of implementation of turbulent shear stress (instead of the semi-empirical Reynolds stress approach of Nezu and Nakagawa, 1993), boundary conditions and initial conditions. For upstream and downstream boundaries zero-order extrapolation method was changed to method of characteristic that behaves well according to the direction of waves (Hirsch, 1998). This model is based on finite volume on a staggered grid with upwind scheme in flux. Steady and unsteady flows can be simulated; different flow regimes such as sub-critical, supercritical, flow discontinuities can be handled. Comparison between measured data (Fukuoka et. al, 2000) and model simulations show good agreement.

2. MODEL DESCRIPTION

2.1 Governing Equations

Two-dimensional depth integrated momentum equations were transformed into natural coordinate system. In addition, by mathematical manipulation using metrics, equation [1a]-[1c] below with contravariant fluxes was obtained.

$$\frac{\partial}{\partial t}\left(\frac{h}{J}\right)+\frac{\partial}{\partial \xi}\left(\frac{Q^{\xi}}{J}\right)+\frac{\partial}{\partial \eta}\left(\frac{Q^{\eta}}{J}\right)=0.0 \qquad [1a]$$

$$\frac{\partial}{\partial t}\left(\frac{Q^{\xi}}{J}\right)+\frac{\partial}{\partial \xi}\left(\frac{UQ^{\xi}}{J}\right)+\frac{\partial}{\partial \eta}\left(\frac{VQ^{\xi}}{J}\right)-\frac{uh}{J}\left(U\frac{\partial \xi_x}{\partial \xi}+V\frac{\partial \xi_x}{\partial \eta}\right)-\frac{vh}{J}\left(U\frac{\partial \xi_y}{\partial \xi}+V\frac{\partial \xi_y}{\partial \eta}\right)=$$

$$-gh\left(\frac{\xi_x^2+\xi_y^2}{J}\frac{\partial z}{\partial \xi}+\frac{\xi_x\eta_x+\xi_y\eta_y}{J}\frac{\partial z}{\partial \eta}\right)-\frac{\tau_b^{\xi}}{\rho J}+\frac{\xi_x^2}{J}\frac{\partial}{\partial \xi}(\tau_{xx}h) \qquad [1b]$$

$$+\frac{\xi_x\eta_x}{J}\frac{\partial}{\partial \eta}(\tau_{xx}h)+\frac{\xi_x^2}{J}\frac{\partial}{\partial \xi}(\tau_{yy}h)+\frac{\xi_y\eta_y}{J}\frac{\partial}{\partial \eta}(\tau_{yy}h)+\frac{\xi_x\eta_y+\xi_y\eta_x}{J}\frac{\partial}{\partial \eta}(\tau_{xy}h)+\frac{2\xi_x\xi_y}{J}\frac{\partial}{\partial \eta}(\tau_{xy}h)$$

$$\frac{\partial}{\partial t}\left(\frac{Q^{\eta}}{J}\right)+\frac{\partial}{\partial \xi}\left(\frac{UQ^{\eta}}{J}\right)+\frac{\partial}{\partial \eta}\left(\frac{VQ^{\eta}}{J}\right)-\frac{uh}{J}\left(U\frac{\partial \eta_x}{\partial \xi}+V\frac{\partial \eta_x}{\partial \eta}\right)-\frac{vh}{J}\left(U\frac{\partial \eta_y}{\partial \xi}+V\frac{\partial \eta_y}{\partial \eta}\right)=$$

$$-gh\left(\frac{\xi_x\eta_x+\xi_y\eta_y}{J}\frac{\partial z}{\partial \xi}+\frac{\eta_x^2+\eta_y^2}{J}\frac{\partial z}{\partial \eta}\right)-\frac{\tau_b^{\eta}}{\rho J}+\frac{\xi_x\eta_x}{J}\frac{\partial}{\partial \xi}(\tau_{xx}h) \qquad [1c]$$

$$+\frac{\eta_x^2}{J}\frac{\partial}{\partial \eta}(\tau_{xx}h)+\frac{\xi_y\eta_y}{J}\frac{\partial}{\partial \xi}(\tau_{yy}h)+\frac{\eta_y^2}{J}\frac{\partial}{\partial \eta}(\tau_{yy}h)+\frac{\xi_x\eta_y+\xi_y\eta_x}{J}\frac{\partial}{\partial \xi}(\tau_{xy}h)+\frac{2\eta_x\eta_y}{J}\frac{\partial}{\partial \xi}(\tau_{xy}h)$$

Where, t is time, h and z (=h+z_b) are water depth and water level elevation respectively, z_b is the ground level elevation, u and v are depth averaged velocities in x and y directions respectively, g is the acceleration due to gravity. The turbulent shear stress terms in x, x-y and y directions are evaluated as in equation [2a] below. The depth averaged turbulent eddy viscosity coefficient, $\boldsymbol{\varepsilon}$ was evaluated by using the commonly used parabolic eddy viscosity formula in [2a] below. This approach has been adopted due to computational ease of application and its contribution to many practical applications. $\boldsymbol{\kappa}$ is the Von Karman constant (=0.41) and u_* is the shear velocity.

$$\tau_{xx}=2\varepsilon\left(\frac{\partial u}{\partial x}\right);\ \tau_{xy}=\tau_{yx}=\varepsilon\left(\frac{\partial u}{\partial y}+\frac{\partial v}{\partial x}\right);\ \tau_{yy}=2\varepsilon\left(\frac{\partial v}{\partial y}\right);\ \varepsilon=\frac{\kappa h u_*}{6};\ u_*=\sqrt{\tau_{bx}/\rho}, \qquad [2a]$$

Expressions for boundary shear stress and Manning's roughness coefficient are shown in [2b]. k_s is the equivalent roughness. The metrics and contravariant velocities (U, V), discharge (Q^{ξ}, Q^{η}) and contravariant boundary shear stress terms ($\tau_b{}^{\xi}$, $\tau_b{}^{\eta}$) are defined as shown in [2c] below.

$$\tau_{bx} = \frac{\rho g n^2 u\sqrt{u^2+v^2}}{h^{1/3}}\ ;\ \tau_{by} = \frac{\rho g n^2 v\sqrt{u^2+v^2}}{h^{1/3}};\ n = h^{1/6}\left(\sqrt{g}\left(6.0+5.75\log_{10}\left(\frac{h}{k_s}\right)\right)\right)^{-1} \quad [2b]$$

$$\xi_x = Jy_\eta;\ \eta_x = -Jy_\xi;\ \xi_y = -Jx_\eta;\ \eta_y = Jx_\xi\ ;\ J = 1/\left(x_\xi y_\eta - x_\eta y_\xi\right)$$

$$U = \xi_x u + \xi_y v;\quad V = \eta_x u + \eta_y v;\quad Q^\xi = \xi_x uh + \xi_y vh;\quad Q^\eta = \eta_x uh + \eta_y vh \quad [2c]$$

$$\tau_b^\xi = \xi_x \tau_{bx} + \xi_y \tau_{by} \text{ and } \tau_b^\eta = \eta_x \tau_{bx} + \eta_y \tau_{by}$$

2.2 Method of solution

Equation [1a] to [1c] above were solved by an explicit numerical scheme that is second order accurate in time and first order accurate in space. The numerical scheme is an improved version Nagata's approach (1999) which uses Adam's Bashforth method (Kreyzig, 1999) and upwind scheme in flux for time and space advancement respectively. Finite volume discretization is employed on a staggered grid arrangement for velocity components in order to avoid pressure discontinuities at the interface. The grid used was non-orthogonal. On the open boundaries (upstream and downstream boundaries), measured discharge hydrograph and measured water depth hydrograph was given respectively. Additionally, on the upstream and downstream boundaries, a unidirectional flow characteristic boundary condition was implemented to compute velocities. For the solid wall boundaries, a slip condition was implemented and no flux crossing through the wall. Wetting and drying was considered by predefining a minimum water depth ($\mathbf{h_{st} = 0.001m}$). When the water depth in the cell under consideration and its surrounding cells was less than $\mathbf{h_{st}}$ then fluxes in that cell during that time step were assigned a value of zero, then computation advanced to next time step. Stability requirement was not explicitly accounted for in the numerical model, time step was chosen sufficiently small and constant throughout the computation time based on trials.

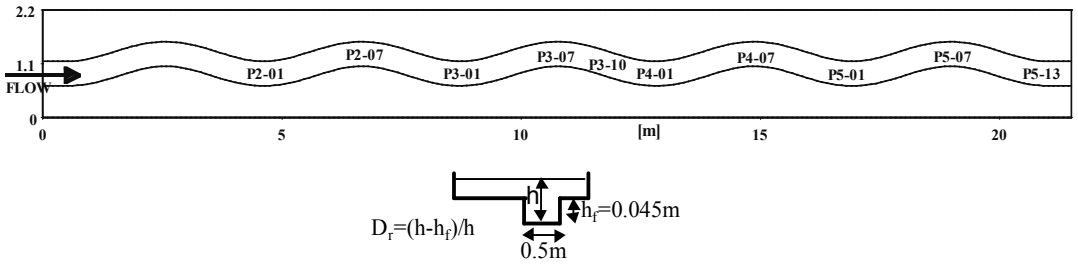

Figure 1 Channel layout plan and measuring points and cross section

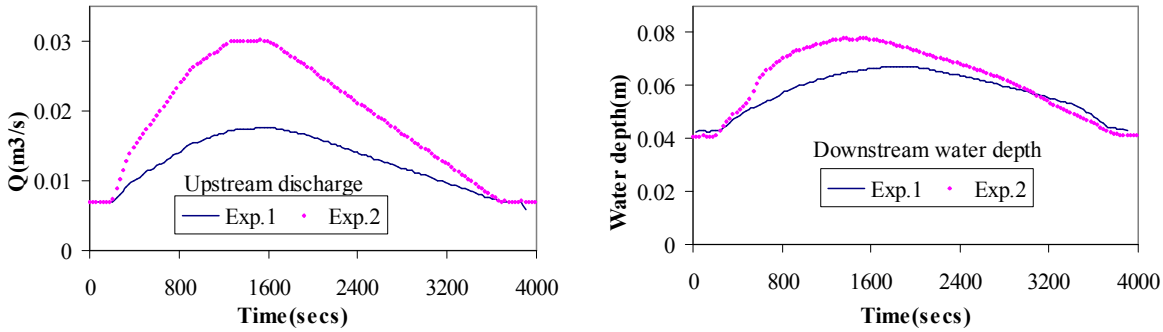

Figure 2 Upstream input discharge hydrograph and downstream water depth hydrograph for Exp.1 and Exp.2

2.3 Model Application

Numerical simulation was done on experimental data (Fukuoka et. al, 2000) for the compound meandering channel shown in Figure 1. The experimental channel was 21.5m long, 0.045m-bankfull depth, and 0.5m wide sine generated main channel with each wavelength

4.1m. Total width of the channel including flood plains was 2.2m and channel slope was 1/500. Measurement points were located at P2-01, P2-07, P3-01, P3-07, P4-01, P4-07, P5-01, P5-07 and P5-13 as indicated in Figure 1. Two sets of experimental runs, Exp.1 and Exp.2 in the same channel conditions were used to verify the simulation results. Measured upstream discharge hydrograph and downstream water depth hydrograph for the respective Exp1 and Exp2, shown in Figure 2 were used as open boundary input conditions in the numerical simulations.

3. RESULTS AND DISCUSSION

3.1 Effect of roughness

In these numerical simulations, water depth on the upstream boundary condition was computed by uniform flow Manning's formula using input discharge hydrograph. The stream-wise velocities for upstream boundary computed by 1-dimensional method of characteristic, required accurate Manning's roughness coefficient distribution with time. Also, in order to obtain accurate upstream boundary water depth from discharge, proper Manning's roughness distribution with time was required. Composite temporal Manning's roughness coefficient for the compound section at the upstream boundary was calculated from measured water surface profiles using one-dimensional non-uniform flow equation. These distributions with time are shown in Figure 4 for Exp.1 and Exp.2.

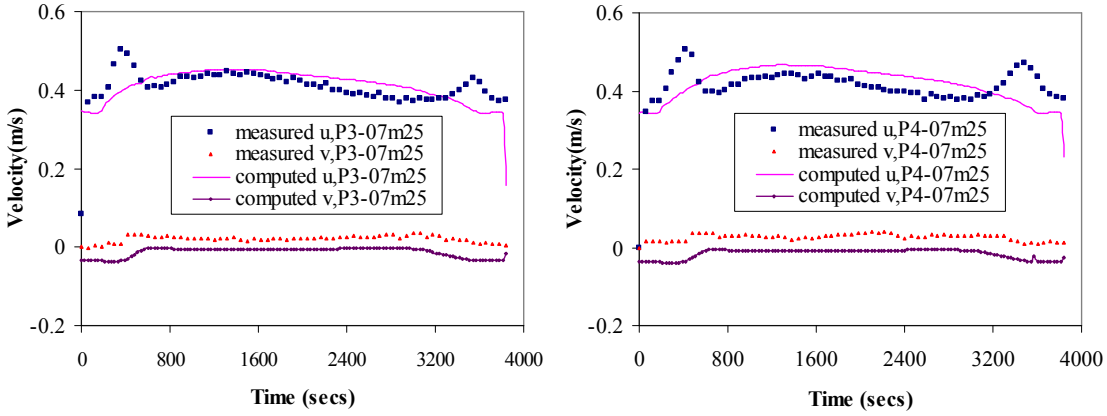

Figure 3 Comparison between measured and simulated velocity hydrographs for Exp1.

3.2 Velocity –hydrographs

Computed velocity hydrographs presented in Figure3 shows discrepancies when relative depth is small ($210s \leq t \leq 600s$ and $3300s \leq t \leq 3800s$). However, the velocity hydrograph of large relative depth coincide well. Three reasons under investigation in this study account for this discrepancy at small relative depths. First, during transition from in-bank flow to over-bank flow, large variations of roughness coefficient account for this discrepancy. In the previous steady flow studies (Myers and Brennan, 1990) roughness variability with relative

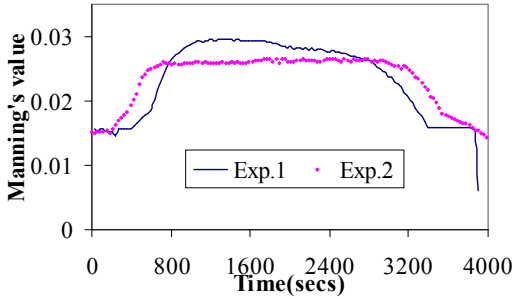

Figure 4 Temporal distribution of upstream Input Manning's roughness coefficient

depth was observed. Second, order 1 upwind schemes are not sufficiently accurate in most practical purposes (Hirsch, 1998). Third, explanation is the depth averaged turbulent eddy viscosity coefficient is inaccurate at the transition from in-bank flow to over-bank flow near the main channel and flood plain interface. This is because of three-dimensional nature of flow in compound channels.

3.3 Water depth-hydrographs

The comparison of experimental and simulated water depth hydrograph results at centerline of the main channel are indicated in Figure 5. Since agreement between the comparison is generally good, the model might be used for prediction of flood wave height, as it propagates

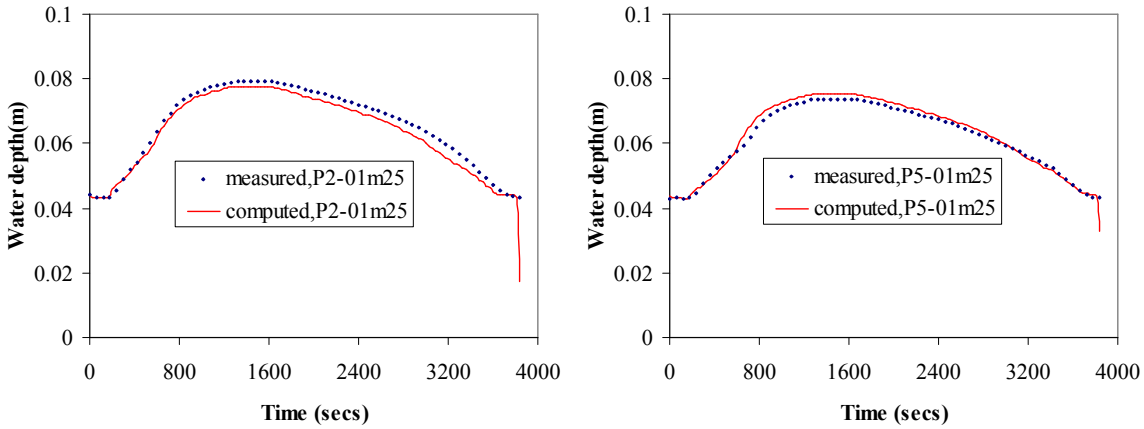

(a) Comparison between measured and simulated water depth hydrograph for Exp1

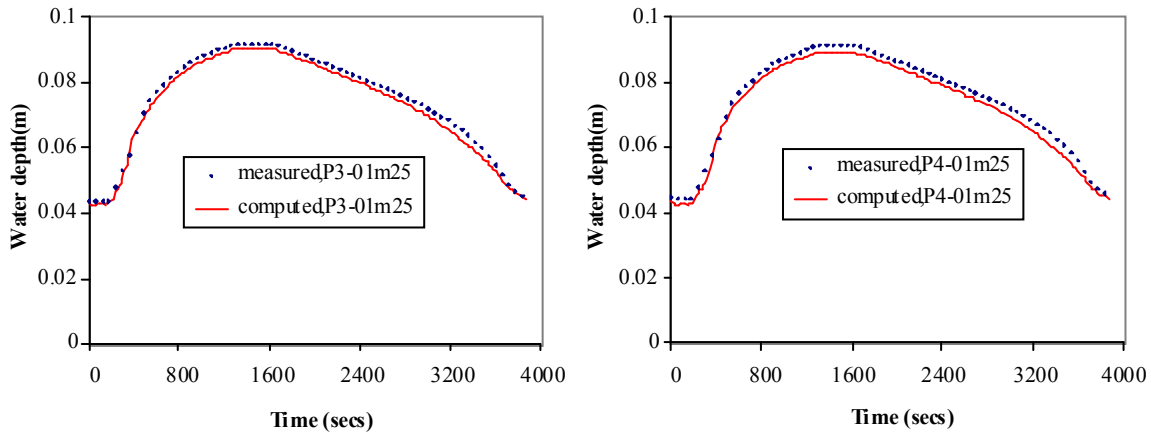

(b) Comparison between measured and simulated water depth hydrograph for Exp2

Figure 5 Comparison between measured and simulated water depth hydrograph

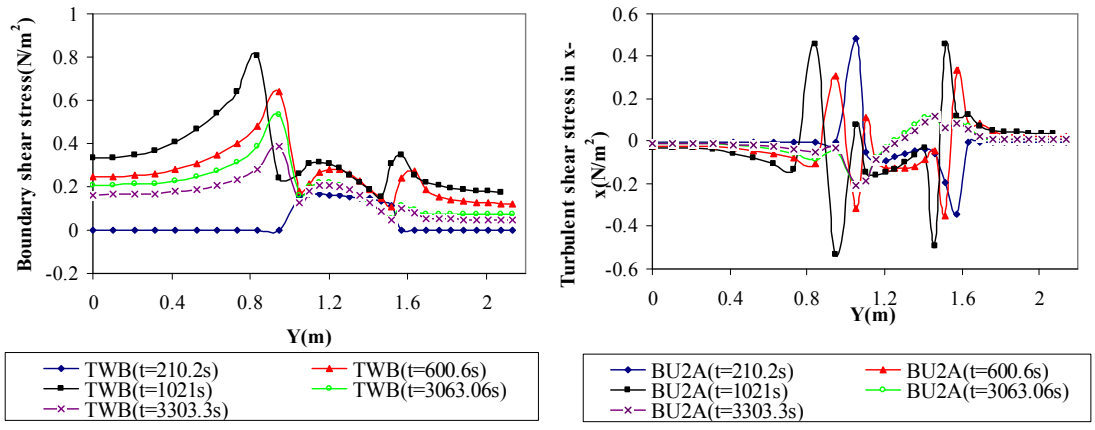

Figure 6 Temporal variation of boundary shear stress and turbulent shear stress in x-x direction (BU2A) at cross section P3-07

in channels. However, for application of the model to natural rivers further investigation is needed.

3.4 Shear stress-hydrographs

From Figure 6, it is clear that maximum values of boundary shear and turbulent shear stress in x-x direction are located around the interface between main channel and flood plain. This occurs when the flow is above bankful ($210s \leq t \leq 3600s$). This shows the interaction between main channel and flood plain when the flow inundates the flood plain. The unsymmetrical pattern of the transverse distribution of the shear stresses arises due to meander channel plan form.

4. CONCLUSION

Comparison between the measured and the simulated water depth hydrographs showed good agreements, this demonstrate how useful the model can be for flood prediction in channels. This unsteady flow study shows additional temporal change of those hydraulic variables and parameters need to be considered during flood flow. The accuracy of upstream and downstream input data is very important for unsteady flow computations.

REFERENCES

1. ASCE Task Committee, 1998, River width adjustment. II: Modeling, Journal of Hydraulic Engineering, ASCE, Vol124-9, pg903-917.
2. Cunge, J A, Holly, F M Jr and Verwey, A, 1980, Practical aspects of computational river hydraulics, Pitman Publishing Limited, London, U.K.
3. Erwin Kreyzig, 1999, Advanced Eng. Mathematics, 8th Edition", John Wiley and Sons
4. Hirsch C,(1994), Numerical Computation of Internal and External Flows, Volume2, Computational methods for Inviscid and Viscous Flows, John Wiley & Sons
5. Fukuoka, S and Watanabe, A, 1998, 3- dimensional analysis on flows in meandering compound channels, Journal of Hydraulic, Coastal and Environmental Eng., JSCE, No586/II-42,pg. 39-50
6. Fukuoka, S, Watanabe, A, Okabe, H and Seki, K, 2000, Effects of Unsteadiness, Plan-form and Cross Sectional form of Channels on Hydraulic Characteristics of Flood Flow, Annual Journal of Hydraulic Engineering, JSCE, Vol.44, pg867-872.
7. Fukuoka S and Fujita K, 1990, Flow resistance due to lateral momentum transport across vegetation in the river course, International Conference on Physical Modeling of Transport and Dispersion, ASCE.
8. Kun-Yeun Han, Jong-Tae Lee, Jae-Hong Park, 1998, Flood inundation analysis resulting from Levee-break, Journal of Hydraulic Research, Vol36-5, pg. 747-759
9. Myers, W R C and Brennan, E K, 1990, Flow Resistance in Compound Channels, Journal of Hydraulic Research, Vol. 28(2), pg. 141-155
10. Nagata, N, Hosoda, T and Muramoto Y, 1999, Characteristics of River Channel Processes with Bank Erosion and Development of Their Numerical Models, Journal of Hydraulic, Coastal and Environmental Engineering, JSCE, Vol. No. 621/II-47, page 23-39
11. Nezu, I and Nakagawa, H, 1993, Turbulence in open channel flows, IAHR Monograph, Balkema, Rotterdam, pg. 53-56
12. Shome M L and Steffler P M, 1998, Lateral flow exchange in transient compound channel flow, Journal of Hydraulic Engineering, ASCE, Vol124-1, pg77-80
13. Sofialidis D and Prinos P, 1998, Compound Open Channel Flow Modeling with Non-Linear Low κ-ε Models, Journal of Hydraulic Engineering, ASCE, Vol124-4, pg253-262
14. Wormleaton P R and Merrett D J, 1990, An improved method of calculation for steady uniform flow in prismatic main channel/flood plain sections, J of Hydr. Research, Vol28-2, pg157-174
15. Zhao D H, Shen H W, Tabios III G Q, Lai J S and Tan W Y, 1994, Finite Volume Two-dimensional Unsteady Flow Model for River Basins, J of Hydr. Eng., ASCE, Vol120-7, p863-883